journal of the mechanical behavior of biomedical materials 140 (2023) 105702

Contents lists available at ScienceDirect

Journal of the Mechanical Behavior of Biomedical Materials

journal homepage: www.elsevier.com/locate/jmbbm

Smooth muscle contribution to vaginal viscoelastic response

Gabrielle L. Clark-Patterson [a], Lily M. Buchanan [b], Benard O. Ogola [c], Maria Florian-Rodriguez [d], Sarah H. Lindsey [e], Raffaella De Vita [f], Kristin S. Miller [a,b,*]

[a] Tulane University, Department of Biomedical Engineering, 6823 St Charles Ave, New Orleans, LA, 70118, USA
[b] University of Texas at Dallas, Department of Bioengineering, 800 W. Campbell Road, Richardson, TX, 75080, USA
[c] Augusta University, Vascular Biology Center, Medical College of Georgia at Augusta University, 1460 Laney Walker Blvd, Augusta, GA, 30912, USA
[d] University of Texas Southwestern Medical Center, Department of Obstetrics and Gynecology, Division of Female Pelvic Medicine and Reconstructive Surgery and Cecil H and Ida Green Center for Reproductive Biological Sciences, 5323 Harry Hines Boulevard, Dallas, TX, 75390-9032, USA
[e] Tulane University School of Medicine, Department of Pharmacology, 1430 Tulane Ave, New Orleans, LA, 70112, USA
[f] Virginia Tech,Department of Biomedical Engineering and Mechanics, 330 A Kelly Hall, 325 Stanger St, Blacksburg, VA, 24061, USA

ARTICLE INFO

Keywords:
Vagina
Smooth muscle cells
Creep
Immunofluorescence
Viscoelastic

ABSTRACT

Smooth muscle cells contribute to the mechanical function of various soft tissues, however, their contribution to the viscoelastic response when subjected to multiaxial loading remains unknown. The vagina is a fibromuscular viscoelastic organ that is exposed to prolonged and increased pressures with daily activities and physiologic processes such as vaginal birth. The vagina changes in geometry over time under prolonged pressure, known as creep. Vaginal smooth muscle cells may contribute to creep. This may be critical for the function of vaginal and other soft tissues that experience fluctuations in their biomechanical environment. Therefore, the objective of this study was to develop methods to evaluate the contribution of smooth muscle to vaginal creep under multiaxial loading using extension – inflation tests. The vaginas from wildtype mice (C57BL/6 × 129SvEv; 3–6 months; n = 10) were stimulated with various concentrations of potassium chloride then subjected to the measured *in vivo* pressure (7 mmHg) for 100 s. In a different cohort of mice (n = 5), the vagina was stimulated with a single concentration of potassium chloride then subjected to 5 and 15 mmHg. A laser micrometer measured vaginal outer diameter in real-time. Immunofluorescence evaluated the expression of alpha-smooth muscle actin and myosin heavy chain in the vaginal muscularis (n = 6). When smooth muscle contraction was activated, vaginal creep behavior increased compared to the relaxed state. However, increased pressure decreased the active creep response. This study demonstrated that extension – inflation protocols can be used to evaluate smooth muscle contribution to the viscoelastic response of tubular soft tissues.

1. Introduction

Smooth muscle cells (SMC) play a significant role in the mechanical function of various soft tissues by controlling the diameter and wall movement through contractions. SMC contractile function is important for various physiological processes such as regulating blood pressure and expelling substances from the body. In addition to contraction, SMCs contribute to soft tissues' quasistatic (Wagner and Humphrey, 2011) and viscoelastic (Greven and Hohorst, 1975; Greven et al., 1976) mechanical behavior. Prior work evaluated SMC contribution to the viscoelastic response uniaxially. However, many tubular soft tissues are subjected to multiaxial loading within the body. Extension-inflation protocols were previously leveraged to subject arteries to multiaxial loading and evaluate SMC contribution to the quasistatic mechanical response (Wagner and Humphrey, 2011). These protocols maintain intact organ geometry and smooth muscle-matrix interactions, which allows the tissue to be subjected to multiaxial loading through axial extension and pressurization. These methods may serve as a useful tool to evaluate SMC contribution to the viscoelastic response of soft tissues under multiaxial loads.

Extension - inflation mechanical testing protocols recently evaluated vaginal viscoelastic response in the passive condition (i.e., no smooth

* Corresponding author. University of Texas at Dallas , Department of Bioengineering and Mechanical Engineering , 800 W. Campbell Road, Richardson, TX, 75080, USA.
E-mail addresses: gclark2@tulane.edu (G.L. Clark-Patterson), Lily.Buchanan@utdallas.edu (L.M. Buchanan), bogola@augusta.edu (B.O. Ogola), Maria.Florian-Rodriguez@UTSouthwestern.edu (M. Florian-Rodriguez), lindsey@tulane.edu (S.H. Lindsey), devita@vt.edu (R. De Vita), Kristin.Miller@utdallas.edu (K.S. Miller).

https://doi.org/10.1016/j.jmbbm.2023.105702
Received 9 November 2022; Received in revised form 22 January 2023; Accepted 1 February 2023
Available online 3 February 2023
1751-6161/© 2023 Elsevier Ltd. All rights reserved.

muscle tone) (Clark-Patterson et al., 2021). However, the vagina is a fibromuscular organ that serves as a canal connecting the uterus to the outside of the body, enabling menstruation, intercourse, and vaginal delivery. The vagina and pelvic structures (i.e., pelvic floor muscles) work together to provide support to the pelvic organs. Vaginal tissue is comprised of extracellular matrix proteins, SMCs, and nerves. The organization and quantity of these components dictate geometry and mechanical function. A continuous baseline contraction maintains vaginal basal tone (Skoczylas et al., 2013). SMCs play a role in sexual arousal, menstruation, and childbirth. During these events, the SMCs relax, increasing vaginal diameter and length (e.g., sexual arousal) allowing the passage of materials (Shafik et al., 2004), or contract, decreasing the diameter and moving materials through the vagina (e.g., sperm, menstruation, fetus) (Fox et al., 1970; Meston et al., 2004; Shafik et al., 2009). Vaginal SMCs undergo significant remodeling with physiologic processes, including pregnancy (Daucher et al., 2007; Ulrich et al., 2014; Rynkevic et al., 2017) and aging (Bortolini et al., 2012). Furthermore, vaginal SMC content significantly decreases in pathologic conditions such as pelvic organ prolapse (Boreham et al., 2002; Takacs et al., 2008). Vaginal delivery subjects the organ to prolonged and increased pressures (Rempen and Kraus, 1991). Likewise, a chronic increase in intra-abdominal pressure (e.g., obesity and excessive heavy lifting) is a risk factor for prolapse (Hendrix et al., 2002; Swift et al., 2003; Jorgensen et al., 1994).

In the nonpregnant vagina, the passive extracellular matrix contributes to changes in vaginal geometry over time under prolonged loads such as pressure, known as creep (Clark-Patterson et al., 2021; Dubik et al., 2022). Creep is a viscoelastic phenomenon that describes the time-dependent increase in deformation (or strain) when a material is subjected to a constant load (or stress). Creep may play a role in supporting the pelvic organs, and vaginal SMCs may contribute to creep by providing pelvic stability and facilitating physiologic processes such as vaginal delivery. However, SMC contribution to vaginal deformation when subjected to sustained pressure remains unknown. Therefore, the objective of this study was to develop methods to evaluate the contribution of smooth muscle to vaginal creep under multiaxial loading using extension – inflation tests.

2. Methods

2.1. Sample collection and experimental set-up

The Institute Animal Care and Use Committee at Tulane University approved all procedures. This study used 15 wildtype female C57BL/6 × 129SvEv at 3–6 months of age at estrus by visual inspection (Byers et al., 2012). All animals were housed under standard housing conditions in a 12-h light/dark cycle at room temperature (20 °C) with free access to food and water. A guillotine euthanized all mice without anesthesia. The vagina was dissected as previously described by White et al. (2019). Two 6-0 sutures per side secured the vagina onto custom 3.75-mm cannulas in an extension-inflation device (Biodynamic 5170 System; TA Instruments Electroforce, New Castle, DE) with the proximal region on the top cannula and the distal end on the bottom (Fig. 1) (Clark-Patterson et al., 2021). After cannulating the vagina and mounting the biochamber, the caps on the top ports of the biochamber were removed to eliminate pressure build-up within the system (Fig. 1). A laser micrometer (Mitutoyo LSM-503S Laser Scan Micrometer with LSM-6200 Display, 2 μm resolution, Mitutoyo Corporation, Kanagawa, Japan) optically tracked the outer diameter at the mid-anterior vaginal wall. Before testing, the laser micrometer was calibrated according to the manufacturer instructions to account for changes between the acrylic biochamber and testing media. A load cell (1000 g; 0.03 g resolution) attached to the top cannula measured load. A linear motor (linear displacement ± 6.5 mm; 1 μm resolution) attached to the bottom cannula axially extended the vagina.

A magnet drive gear pump (I-Drive model 76003; Micro pump Inc., Vancouver, WA) in a closed feedback loop with a pressure transducer placed in the lumen of the vagina (3.5F Mikro-Cath Part # 825–0101, 500 mmHg/67 kPa maximum pressure, accuracy ± 0.5 mmHg/0.07 kPa, Millar, Texas, USA) controlled and measured pressure. This pump is shown in Fig. 1 as pump 1. An adjustable clamp attached to the downstream tube controlled the pump drive. Wintest software was used to control the pump pressure and the linear motor (TA Instruments Electroforce, Delaware, USA).

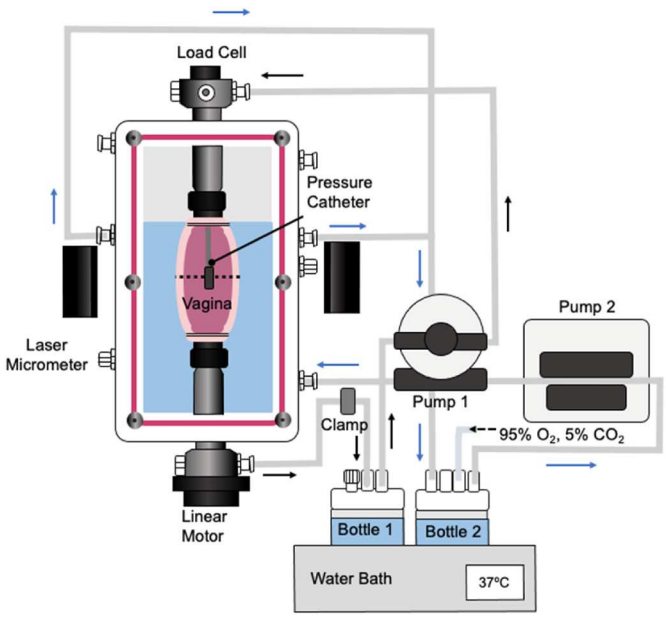

Fig. 1. A water bath, second bottle, and second pump were added to the Electroforce set-up to permit active testing under 37 °C with carbogen aeration to maintain pH levels. A tube was connected to bottle 2 then through pump 2 to the bottom port on the chamber. Two tubes connected with a "Y" connector allowed fluid to exit the biochamber returning to media to bottle 2 creating a continuous flow loop. Carbogen was bubbled into bottle 2. The blue lines show the flow loop through the biochamber. The black line shows the flow loop through the cannula. Pump 1 flows through the cannula in a feedback loop with the pressure catheter to control pressure applied to the vagina.

Extension-inflation protocols previously evaluated the passive creep response of the murine vagina at room temperature (Clark-Patterson et al., 2021). Modifications to the extension – inflation system permitted assessment of creep on freshly isolated vaginal tissue, maintaining smooth muscle contractile function over time. A secondary peristaltic pump (MasterFlex L/S Easy-Load Peristaltic Pump; Cole Palmer, Vernon Hills, IL) continuously circulated Krebs Ringer Buffer (KRB; 120 mM NaCl, 25 mM $NaHCO_3$, 4.7 mM KCl, 2.5 mM $CaCl_2$, 1.2 mM NaH_2PO_4, 1.2 mM $MgCl_2$, 11 mM glucose) through the biochamber near 37 °C (Clark et al., 2019; Murtada et al., 2016). This pump is shown in Fig. 1 as pump 2. A water bath heated the testing media throughout the test, and 95% oxygen and 5% carbon dioxide aerated the media to maintain pH near 7.4. A pilot study assessing contractility over 3 h demonstrated that time did not significantly affect contractility.

2.2. Active creep testing

Immediately after euthanasia, the vagina was dissected and secured in the extension-inflation device in KRB (n = 10) (Clark-Patterson et al., 2021). The length and pressure at which the vagina slightly buckled but did not collapse identified the unloaded configuration (White et al., 2019; Clark et al., 2019; Robison et al., 2017; Akintunde et al., 2019). A 4-mmHg (0.53 kPa) tare pressure prevented the vagina from collapsing to allow consistent and repeatable mechanical tests (White et al., 2019; Clark et al., 2019; Robison et al., 2017; Akintunde et al., 2019).

Potassium chloride (KCl) was used to pre-expose or precondition the vagina to the stimuli used throughout the test. KCl induces muscle contraction through direct membrane depolarization, resulting in a simple and repeatable mechanism of contraction-independent of neural function and the number of available receptors (Skoczylas et al., 2013; Clark et al., 2019; Jallah et al., 2016). This study used 40 mM KCl because this concentration induced maximum tonic contraction in the murine vagina (Clark et al., 2019). To ensure viability and avoid any deformation caused by pressure, 40 mM KCl stimulated the vagina without pressure at unloaded length (Fig. 2A). The vagina contracted for 300 s to achieve a constant maximum contractile response (Clark et al., 2019; Jallah et al., 2016), and was then washed with fresh KRB to return the SMC to the basal state over another 300-s period.

After smooth muscle preconditioning, the experimental physiologic length was determined (White et al., 2019; Clark et al., 2019; Robison et al., 2017; Akintunde et al., 2019). During dissection, the vagina retracts or shortens in length due to removing the natural *in vivo* tethering (White et al., 2019; Clark et al., 2019; Robison et al., 2017; Akintunde et al., 2019). Initial estimations of vaginal retractions were made by measuring the *in vivo to ex vivo* change in vaginal axial length (White et al., 2019; Robison et al., 2017; Amin et al., 2012). Methods were adapted from extension-inflation testing used within vasculature, to further estimate the physiologic length experimentally. In blood vessels, at the experimental physiologic length, the load remains constant over a range of increasing pressures to preserve energy (Vanloon et al., 1977; Weizsacker et al., 1983; Ferruzzi et al., 2013). Herein, the experimental physiologic length was determined where load remained constant from 0 to 15 mmHg (Fig. 3A) (White et al., 2019; Robison et al., 2017; Akintunde et al., 2019). During pressurization the tissue was fixed axially, and the load cell measured load at the fixed length.

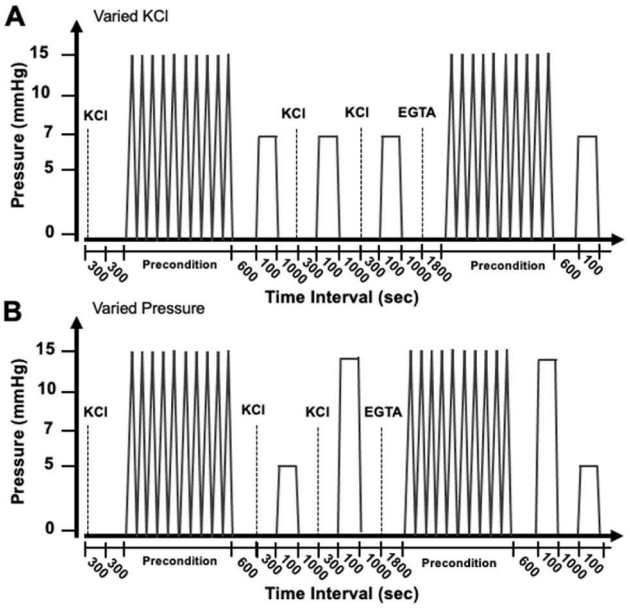

Fig. 2. Schematic of active and passive creep experimental methods in response to various KCl concentrations (A). Schematic of pressure-dependent active and passive creep experimental methods (B). At the unloaded length and no pressure, the SMCs were pre-exposed to 40 mM potassium chloride (KCl) for 300 s. The high KCl solution was replaced with fresh media to return to the basal state. Ten cycles of pressurization preconditioned the vagina at the physiologic length followed by a 600-s equilibration period. For the varied KCl protocol, the vagina was randomly stimulated with various concentrations of KCl (4.7, 20, and 40 mM) then subjected to 7 mmHg. For the varied pressure protocol, the vagina was stimulated with 40 mM KCl then randomly subjected to 5 and 15 mmHg. Creep was evaluated for 100 s with a 1000-s recovery period. The randomization is not depicted in this figure. Egtazic acid (EGTA) relaxed the SMCs, then creep testing was repeated in the passive state.

Ten cycles of pressurization from 0 to 15 mmHg (0–2 kPa) at the determined physiologic length preconditioned the vagina to obtain a consistent and repeatable mechanical response (Fig. 2A) (Clark-Patterson et al., 2021; Robison et al., 2017). The rate of pressurization (1.5 mmHg/s; 0.2 kPa/s) was controlled by the device using the Wintest software (Clark-Patterson et al., 2021; Robison et al., 2017). The vagina equilibrated at the physiologic length under no pressure for 10 min (Clark-Patterson et al., 2021), then underwent 3 randomized active creep tests: smooth muscle basal tone (4.7 mM KCl baseline concentration in KRB (Wanggren et al., 2008; Hong et al., 2019; Caulk et al., 2019)), contracted with 20 mM KCl, and contracted with 40 mM KCl (Fig. 2). 20 mM KCl was selected because it was one-half of the concentration that induced maximum contraction (40 mM) (Clark et al., 2019). Using various concentrations of KCl enabled assessment of how the degree of contraction affected creep. Random allocation was performed to minimize any artifacts that may be attributed to the order of SMC stimulation. The vagina was contracted with KCl for 300 s, then the pressure was increased to the mean *in vivo* pressure of 7 mmHg (0.93 kPa), as previously measured by balloon pressure catheterization (Fig. 2A) (Clark et al., 2021).

The pressure was held constant for 100 s and then removed for 1000 s of recovery (Clark-Patterson et al., 2021; Provenzano et al., 2001; Hingorani et al., 2004). Immediately after removing the pressure, the media was replaced with fresh KRB to return the vagina to the basal state. The recovery period was 10 times longer than the duration of the creep test as previously recommended (S, 1973). A previous study demonstrated that repeated 100-s creep test with 1000 s of recovery did not significantly affect the creep response in the mouse vagina (Clark--Patterson et al., 2021). Although 100 s of creep does not fully describe the vaginal creep behavior (primary and secondary), it provides an initial analysis and allows multiple creep tests on the same sample (Clark et al., 2021). During active creep, 6 of the 10 samples spontaneously contracted during the creep test. When this occurred, pressure was immediately removed and following a recovery period, the test was repeated. This was primarily observed with contraction using 20 mM KCl, and the spontaneous contraction occurred immediately following pressurization to the mean *in vivo* pressure. After the 3 active creep tests, the vagina was treated with 2 mM egtazic acid for 1800 s (30 min) in KRB without calcium to remove the smooth muscle tone (Clark et al., 2019). After treatment, the media was replaced with fresh KRB without calcium. The vagina then underwent preconditioning (10 cycles of pressurization) and equilibration followed by a creep cycle under passive (no muscle tone) condition (Fig. 2A).

2.3. Pressure-dependent active creep

The methods developed to assess the smooth muscle contribution to creep were then extended to assess how this creep behavior changed with increased pressure. This study evaluated creep with smooth muscle contractility and in a passive state in response to 5 mmHg (0.67 kPa) and 15 mmHg (2 kPa) of constant pressure (Fig. 2B). Pressures of 5 and 15 mmHg were selected due to a previous study in the murine vagina that showed an increase in creep strain under 15 mmHg compared to 5 mmHg in the passive state (Clark-Patterson et al., 2021). Further, 5 mmHg was one standard deviation below the mean measured *in vivo* vaginal pressure and 15 mmHg is near double the mean *in vivo* pressure (7 mmHg) (Clark-Patterson et al., 2021). That doubling reflects the two-fold increase in intravaginal pressure previously quantified in humans during normal daily activities such as lying down, standing or sitting up, and walking (Kruger et al., 2013). Immediately after euthanasia, the vagina (n = 5) was dissected and secured in the extension-inflation device in KRB. The unloaded configuration (length and pressure) was identified when the vagina slightly buckled but did not collapse (4 mmHg) (White et al., 2019; Clark et al., 2019; Robison et al., 2017; Akintunde et al., 2019). KCl was used to pre-expose or precondition the vagina's SMCs under low loads to ensure viability (as

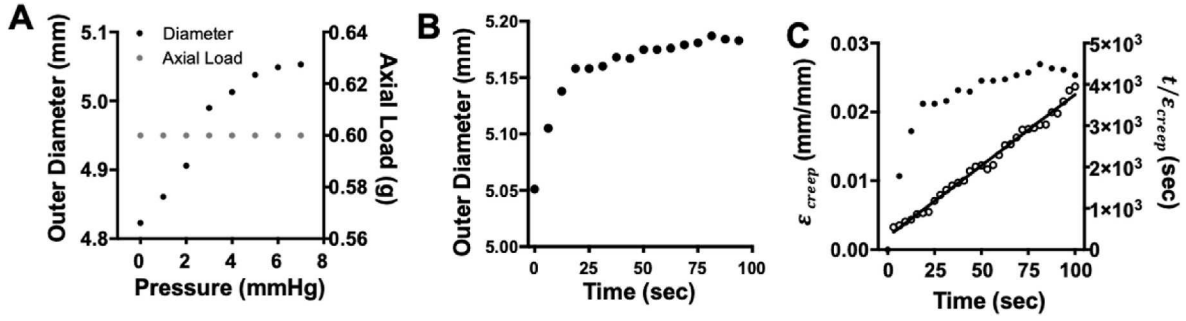

Fig. 3. Representative outer diameter (black) and axial load (grey) response to increasing pressure (A). Representative outer diameter curve over 100 s of creep under a constant 7 mmHg (B). Representative strain (filled; left y-axis) versus time curve for 100 s of creep (C). Peleg's equation linearly transformed the strain versus time response (open; right y-axis) and a linear regression determined the slope and intercept of the linear line (black line). Outer diameter and creep strain are reported every 6 s for visualization. The linearly transformed curve is reported every 3 s demonstrating data analysis.

previously described in Section 2.2). The experimental physiologic length was identified, where the load remained constant under increasing pressure (Vanloon et al., 1977; Weizsacker et al., 1983). Ten cycles of pressurization (0–15 mmHg; 1.5 mmHg/s) at the physiologic length preconditioned the vagina to obtain a consistent and repeatable response (Clark-Patterson et al., 2021). The vagina equilibrated at the physiologic length under no pressure for 600 s.

At physiologic length, 40 mM KCl contracted the vagina for 5 min. The 40 mM KCl concentration was selected because it generated maximum tonic contractions and significantly contributed to creep compared to the passive condition (Clark et al., 2019). The basal condition did not statistically significantly contribute to creep compared to the passive condition and 20 mM KCl resulted in a spontaneous contraction during creep. The pressure was then randomly increased to 5 or 15 mmHg for 100 s of creep. Random allocation was carried out to minimize any artifacts that may be due to the order that the load was applied (Clark-Patterson et al., 2021). The pressure was removed for 1000 s of recovery. Immediately after removing pressure, the media was replaced with fresh KRB, returning the vagina to the basal state. This protocol was repeated at the remaining randomly allocated target pressure (5 or 15 mmHg). After the two active creep tests, the vagina was treated with 2 mM of egtazic acid for 30 min in KRB with no calcium to remove the smooth muscle tone (Clark et al., 2019). After treatment, the media was replaced with fresh KRB without calcium. The vagina underwent preconditioning and equilibration. At the physiological length, the pump randomly increased pressure to 5 or 15 mmHg for 100 s of creep. The pressure was removed for 1000 s of recovery. This protocol was repeated at the remaining randomly allocated target pressure (5 or 15 mmHg).

2.4. Creep and contractility data analysis

Creep strain was quantified by normalizing the outer diameters (d_o) to the reference outer diameter at 0 s (Eqn. (1); Fig. 3B). Zero seconds ($t = 0$) denoted the start of the experiment when the pressure reached 7 mmHg (or the target pressure). This excluded the changes in diameter due to the elastic response (Asundi and Rempel, 2008; Thornton et al., 2000, 2002). This was selected as the reference for this study to compare the accumulation of deformation across active loading conditions (Clark-Patterson et al., 2021). Peleg's equation transformed the nonlinear strain vs. time curve to a linear relationship by dividing time by strain to compare the creep data (Eqn. (2); Fig. 3C) (Peleg, 1979a).

$$t/\varepsilon_{creep}(t) = k_1 + k_1 t \tag{2}$$

$$\varepsilon_{creep} = \frac{d_o(t) - d_o(0)}{d_o(0)} \tag{1}$$

This method recently described stress-relaxation in swine vaginas (Pack et al., 2020) and creep (Clark-Patterson et al., 2021) in rodent vaginas. A linear regression determined Peleg's constants k_1 and k_2. The reciprocal of k_1 describes the initial rate of creep at time equals 0 s. The reciprocal of constant k_2 represents the hypothetical asymptotic level for strain as time approaches infinity (Peleg, 1979a, 1979b). Analysis was performed every 3 s from 0 to 100 s. Data are reported every 6 s for visualization (Fig. 3C).

For the active creep test (as described in section 2.2) the percent change between the passive and contracted (basal, 20 mM KCl and 40 mM KCl) outer diameters (OD; Eqn. (3)) quantified the degree of circumferential contraction (Eqn (3)) (Ramachandra and Humphrey, 2019). For each test, the contracted (basal, 20 mM KCl and 40 mM KCl) outer diameter was individually compared to the passive outer diameter at the start of the creep test ($t = 0$) under the mean *in vivo* pressure (7 mmHg). For pressure-dependent active creep test (as described in section 2.3) the percent change between the passive and contracted (40 mM KCl) outer diameters (OD; Eqn. (3)) quantified the degree of circumferential contraction (Eqn. (3)) (Ramachandra and Humphrey, 2019). The contracted (40 mM KCl) outer diameter was compared to the passive outer diameter at the start of the creep test ($t = 0$) under 5 mmHg. The contracted (40 mM KCl) outer diameter was compared to the passive outer diameter at the start of the creep test ($t = 0$) under 15 mmHg.

$$\%\Delta Outer\ Diameter = \frac{OD_{contracted} - OD_{passive}}{OD_{passive}} x100 \tag{3}$$

2.5. Immunofluorescence

After active creep testing (as described in section 2.2), 10% formalin perfusion fixed the vaginas ($n = 6$) at the physiologic length and mean *in vivo* pressure (7 mmHg) for 24 h. The samples were embedded in paraffin. A circumferential section of 4 μm thickness was taken from the middle region of the vagina and then placed on glass slides. The slides were heated at 55 °C for 1 h followed by washes in xylene, 100% and 70% alcohol, and tris buffered saline solution, respectively. The slides were then incubated in methanol-hydrogen peroxide mixture for 30 min (98:1). Heat antigen retrieval was performed in Rodent Decloaker (cat#RD913 L, Biocare Medical, California, USA) for 30 min at 98 °C followed by distilled water rinsing. Pap pen was used to demarcate around tissue sections followed by background sniper for 20 min (cat#BS966 H, Biocare Medical, California, USA). Primary antibody incubations were performed overnight at the following dilutions: myosin heavy chain (MHC; 1:100; cat# ab124679, Abcam, Cambridge, United Kingdom) and alpha smooth muscle-actin (α SMA; 1:100; cat# 14-9760-82, Thermo Fisher Scientific, Massachusetts, USA). Slides were washed in TBST four times for 5 min followed by secondary antibody incubation for 2 h at room temperature at the following dilutions: anti-rabbit-MHC (1:500) and anti-mouse-Alpha Actin (1:500). The slides were washed in TBST four times for 5 min followed by an application of mountant and DAPI (Cat# P36935, Invitrogen, Massachusetts, USA).

The slides were allowed 24 h to dry before imaging.

Images were taken at 20x magnification (400 × 295μm) on the BioTek Cytation-5 Imaging System (Agilent Technologies, California, USA). One section per animal was imaged with three random images per section. A custom MATLAB code manually counted the cells within the muscular layer expressing α SMA and/or MHC. ImageJ quantified the cross-sectional area of the muscular layer. The number of SMCs was normalized to the muscularis cross-sectional area. All three images per section were analyzed and then averaged to obtain a single value for the section.

2.6. Statistics

A Shapiro-Wilk normality test evaluated the normal distribution of the data. A one-way ANOVA or nonparametric Kruskal-Wallis test evaluated the effect of smooth muscle tone on Peleg's constants, initial creep rate, and creep strain at 100 s, with Tukey's or Dunn's post hoc test when necessary. Multiple paired *t*-test evaluated the percent change in outer diameter between the various levels of smooth muscle stimulation (basal, 20 mM, and 40 mM) with Bonferroni correction ($p < 0.05/2 = 0.025$). A Pearson's or nonparametric Spearman's test evaluated the correlation between the percentage change in the outer diameter versus initial creep rate and creep strain at 100 s. T-test or the nonparametric Mann-U Whitney test evaluated the effect of pressure on creep (Peleg's constant, creep rate and creep strain) between 5 and 15 mmHg in the contracted (40 mM KCl) and passive states. A Pearson's correlation evaluated the relationship between the number of SMCs normalized to cross-sectional area versus the percentage change in the outer diameter, initial creep rate, and creep strain at 100 s. All data was used in the statistical analysis.

3. Results

3.1. Smooth muscle contribution to creep

The creep strain curve shifted upwards with basal tone and when contracted with 20 and 40 mM KCl compared to the passive creep strain curve (Fig. 4A). A one-way ANOVA or nonparametric Kruskal-Wallis test showed that smooth muscle contraction significantly affected Peleg's constant k_1 ($p < 0.001$), Peleg's constant k_2 ($p < 0.001$), initial creep rate ($p < 0.001$), and creep strain at 100 s ($p = 0.005$). Contraction with 20 mM KCl significantly decreased Peleg's constant k_1 ($p = 0.02$), decreased Peleg's constant k_2 ($p < 0.001$), increased initial creep rate ($p = 0.02$), and increased creep strain at 100 s ($p < 0.001$) compared with the passive state (Table 1). Contraction with 40 mM KCl significantly decreased ($p < 0.001$) Peleg's constant k_1, decreased Peleg's constant k_2, increased initial creep rate and increased creep strain at 100 s compared to the passive state. Contraction with 40 mM KCl significantly decreased constant Peleg's k_1 ($p = 0.004$), increased initial creep rate ($p = 0.004$), and increased creep strain at 100 s ($p = 0.03$) compared with the basal state.

Table 1
Peleg's constants, initial creep rate, and creep strain at 100 s of creep (n = 10). Data is reported as mean ± SEM.

	Basal	20 mM	40 mM	Passive
k_1 (x10^2, sec)	34 ± 5	6 ± 1[a]	3 ± 1[a,b]	40 ± 10
k_2 (−)	89 ± 25	30 ± 7[a]	24 ± 5[a]	202 ± 56
R^2	0.85 ± 0.04	0.83 ± 0.06	0.98 ± 0.01	0.92 ± 0.03
Initial Creep Rate (x10^{-3}, sec^{-1})	1.43 ± 0.61	1.90 ± 0.22[a]	4.17 ± 0.64[a,b]	0.41 ± 0.12
Creep Strain (x10^{-2}, mm/mm)	1.93 ± 0.66	3.65 ± 0.63[a]	4.79 ± 0.76[a,b]	0.67 ± 0.16

[a] Denotes $p < 0.05$ compared to passive.
[b] Denotes $p < 0.05$ compared to basal.

Contraction with 40 ($p < 0.001$) and 20 ($p = 0.007$) mM KCl increased the percentage change in the outer diameter compared to the basal state (Fig. 5A). The percentage is negative due to decease in diameter with contraction. Contraction with 40 mM KCl increased ($p = 0.006$) the percentage change in the outer diameter compared to 20 mM KCl. A Spearman's correlation demonstrated that the percent change in the outer diameter significantly negatively correlated ($\rho = -0.59$; $p < 0.001$) with creep strain at 100 s (Fig. 5B). A Spearman's correlation demonstrated that the percent change in the outer diameter significantly negatively correlated ($\rho = -0.47$; $p = 0.008$) with the initial creep rate (Fig. 5C). This demonstrated a greater creep response with a greater decrease in the outer diameter due to smooth muscle contraction.

3.2. The effect of pressure on smooth muscle contractility and creep

Under 15 mmHg, the creep versus strain curve shifted downward with smooth muscle contraction (Fig. 6A) and slightly upwards without smooth muscle contraction (passive). With the smooth muscle contraction, Peleg's constants k_1 ($p = 0.04$) and k_2 ($p = 0.02$) increased under 15 mmHg compared to 5 mmHg (Table 2), and the initial creep rate ($p = 0.04$) and creep strain at 100 s ($p = 0.02$) decreased under 15 mmHg compared to 5 mmHg. Without smooth muscle contraction (passive), creep strain at 100 s increased ($p = 0.04$) at 15 mmHg compared to 5 mmHg, however, there was no significant impact on Peleg's constants.

The percent change in the outer diameter decreased significantly ($p = 0.03$) under 15 mmHg compared to 5 mmHg (Fig. 7A). A Pearson's correlation demonstrated that the percent change in the outer diameter significantly negatively correlated with creep strain at 100 s ($r = -0.92$;

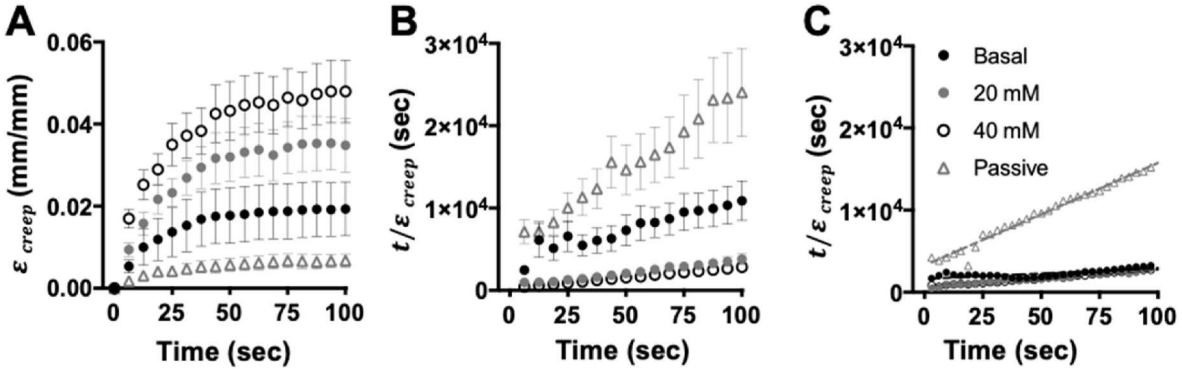

Fig. 4. Creep strain versus time curves (A) for the basal response (black filled circle), contracted with 20 (grey filled circle) and 40 (black open circle) mM KCl, and passive (grey open triangle) in wildtype controls (n = 10). The creep strain curve shifted upward with smooth muscle contraction compared to the passive state. Linear transformed curve using Peleg's equation (B). Representative Peleg's linearized curves and linear regression (dashed line) with the data reported every 3 s as performed for analysis (C). Data are reported as mean ± SEM.

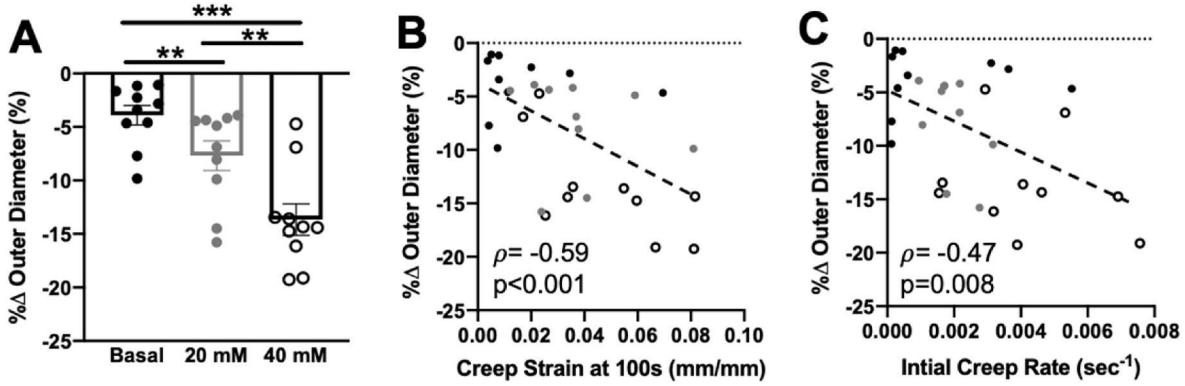

Fig. 5. Percent change in outer diameter (A) for the basal (black filled circle), 20 mM KCl (grey filled circle) and 40 mM KCl (black open circle) contractile response in wildtype control vaginas (n = 10). The negative sign denotes a decrease in outer diameter with contraction. Contractility was greater at 40 and 20 mM KCl compared to the basal response. Contractility was greater at 40 mM KCl compared to 20 mM KCl. Percent change in outer diameter versus creep strain at 100 s (B). The percent change in outer diameter significantly negatively correlated with creep strain at 100 s. Percent change in outer diameter versus the initial creep rate (C). The percent change in outer diameter significantly negatively correlated with the initial creep rate. The dashed line represents the best-fit line for the correlation. Data are reported as mean ± SEM. Statistical significance is denoted as **p < 0.01 and ***p < 0.001.

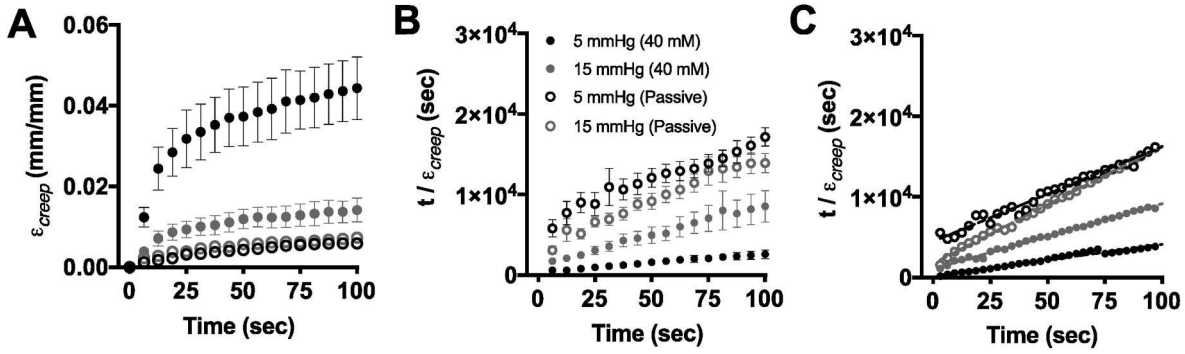

Fig. 6. Creep strain versus time curves (A) at 5 (black filled circle) and 15 (grey filled circle) mmHg when contracted and at 5 (black open circle) and 15 (grey open circle) mmHg when passive in wildtype controls (n = 5). The creep strain curve shifted downwards at 15 mmHg with smooth muscle contraction compared to 5 mmHg. The creep strain curve slightly shifted upwards at 15 mmHg without smooth muscle contraction compared to 5 mmHg. Linear transformed curve using Peleg's equation (B). Representative Peleg's linearized curves and linear regression (dashed line) with the data reported every 3 s as performed for analysis (C). Data are reported as mean ± SEM.

Table 2
Peleg's constants, initial creep rate, and creep strain at 100 s for pressure-dependent creep (n = 5). Data is reported as mean ± SEM.

	5 mmHg (40 mM)	15 mmHg Active (40 mM)	5 mmHg (Passive)	15 mmHg (Passive)
k_1 (x10^2, sec)	4 ± 2	12 ± 3[a]	64 ± 15	32 ± 8
k_2 (–)	22 ± 5	76 ± 22[a]	105 ± 21	111 ± 20
R^2	0.97 ± 0.01	0.97 ± 0.01	0.89 ± 0.05	0.92 ± 0.04
Initial Creep Rate (x10^{-3}, sec^{-1})	3.72 ± 1.11	1.08 ± 0.24[a]	0.21 ± 0.06	0.43 ± 0.12
Creep Strain (x10^{-2}, mm/mm)	4.44 ± 0.78	1.43 ± 0.30[a]	0.59 ± 0.03	0.74 ± 0.07[b]

[a] Denotes p < 0.05 compared to 5 mmHg 40 mM KCl.
[b] Denotes p < 0.05 compared to 5 mmHg Passive.

p = 0.003; Fig. 7B). A nonparametric Spearman's correlation demonstrated that the percent change in outer diameter significantly negatively correlated with initial creep rate (ρ = -0.72; p = 0.02; Fig. 7C). This demonstrated a greater creep response with a greater decrease in the outer diameter due to smooth muscle contraction.

3.3. Vaginal smooth muscle immunofluorescent analysis

In the muscularis the cells expressed α SMA (Fig. 8B) and MHC (Fig. 8C). Blood vessels in the subepithelium and adventitia also expressed α SMA and MHC. In four of the six samples, the SMCs near the adventitia layer were elongated and the cells near the subepithelium were more circular. A Pearson's correlation evaluated the relationship between the number of SMCs normalized to the muscularis cross-sectional area versus to the percent change in diameter when maximally contracted with 40 mM KCl (black open circle data in Fig. 5A). A Pearson's correlation also evaluated the relationship between the number of SMCs normalized to the muscularis cross-sectional area versus the creep behavior when maximally contracted with 40 mM KCl (data in Table).

The Pearson's correlation did not detect a significant correlation between the number of cells in the muscularis expressing α SMA and/or MHC normalized to the cross-sectional area of the muscularis versus the percent change in the outer diameter with contractility (r = -0.49; p = 0.35; Fig. 9A). The Pearson's correlation did not detect a significant correlation between the number of cells in the muscularis expressing α SMA and/or MHC normalized to the muscularis cross-sectional area versus creep strain at 100 s (r = -0.18; p = 0.74; Fig. 9B). The Pearson's correlation did not detect a significant correlation between the number of cells in the muscularis that express α SMA and/or MHC normalized to the muscularis cross-sectional area versus initial creep rate (r = -0.29; p

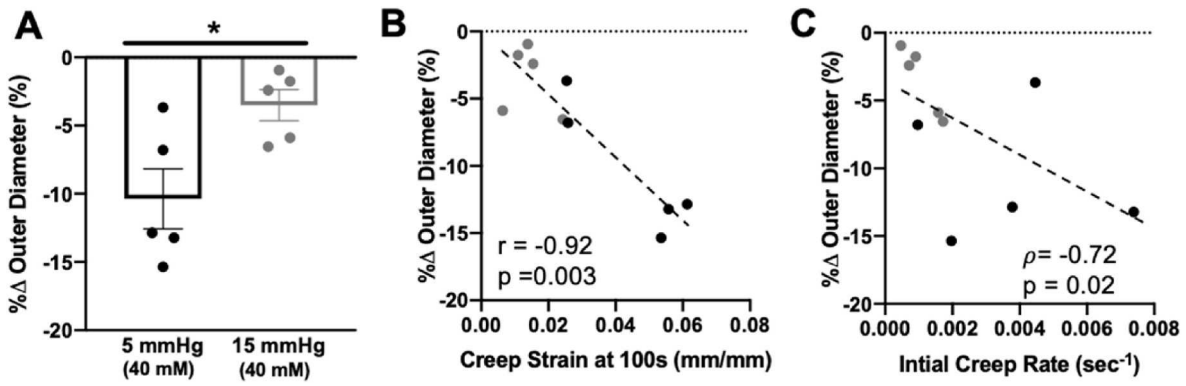

Fig. 7. Percent change in outer diameter (A) at 5 (black filled circle) and 15 (grey filled circle) mmHg when contracted with 40 mM KCl in wildtype controls (n = 5). The negative sign denotes a decrease in outer diameter with contraction. Contractility decreased under 15 mmHg compared to 5 mmHg. The percent change in outer diameter versus creep strain at 100 s (B). The percent change in outer diameter significantly negatively correlated with creep strain at 100 s. Percent change in outer diameter versus the initial creep rate (C). The percent change in outer diameter significantly negatively correlated with the initial creep rate. The dashed line represents the best-fit line for the correlation. Data are reported as mean ± SEM. Statistical significance is denoted as *p < 0.05.

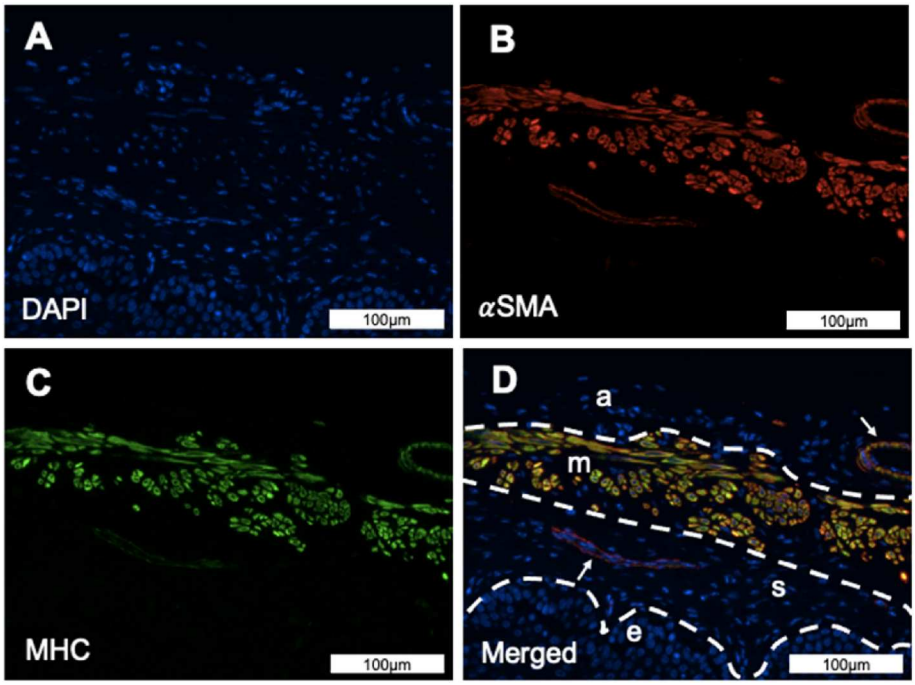

Fig. 8. Representative DAPI (blue; A) image staining for the cellular nuclei, alpha-smooth muscle actin staining (α SMA, red; B), and myosin heavy chain (MHC, green; C). Merged immunofluorescent image (yellowish orange) of the murine vaginal wall (D). The layers of the vaginal wall are denoted as: epithelium (e), subepithelium (s), muscularis (m), and adventitia (a). The white dashed line separates the layers. The arrows identify the blood vessels. The scale is 100 μm.

= 0.57; Fig. 9C).

4. Discussion

This study developed experimental methods to evaluate SMC contribution to the viscoelastic properties of tubular soft tissues under multiaxial loading. SMCs undergo significant remodeling with physiologic processes, such as aging (Bortolini et al., 2012; Vazquez-Padron et al., 2004; Fritze et al., 2012)and pathologic conditions (Boreham et al., 2002; von Kleeck et al., 2021). SMCs viscoelastic contribution to these processes and to daily function is poorly understood. Understanding SMC function may aid in developing tools to elucidate their role in physiologic and pathologic conditions. This study evaluated creep in the healthy murine vagina. It demonstrated that smooth muscle tone increased the creep response and the degree of contraction positively correlated with creep strain and rate. The authors found this surprising. It was speculated that activation of SMCs would play a role in maintaining vaginal diameter. Further, that a loss in SMCs tone may contribute to an increase in vaginal diameter over time and play a role in pathologic conditions, such as pelvic organ prolapse. This finding, however, was similar to results in the guinea pig colon, where smooth muscle contraction increased creep strain (Greven and Hohorst, 1975; Greven et al., 1976). Basal muscle tone, however, did not statistically significantly affect creep compared with the passive response. Previous work demonstrated that basal muscle tone significantly contributed to the quasi-static mechanical response in the murine vagina by decreasing material stiffness (Clark et al., 2019). This may suggest that basal muscle tone is more important for the instantaneous mechanical response that allows the vagina to expand under a continuous increase in pressure.

This study also demonstrated that an increase in pressure (5 vs. 15 mmHg) with smooth muscle tone significantly decreased the creep response. However, under passive conditions, creep strain mildly

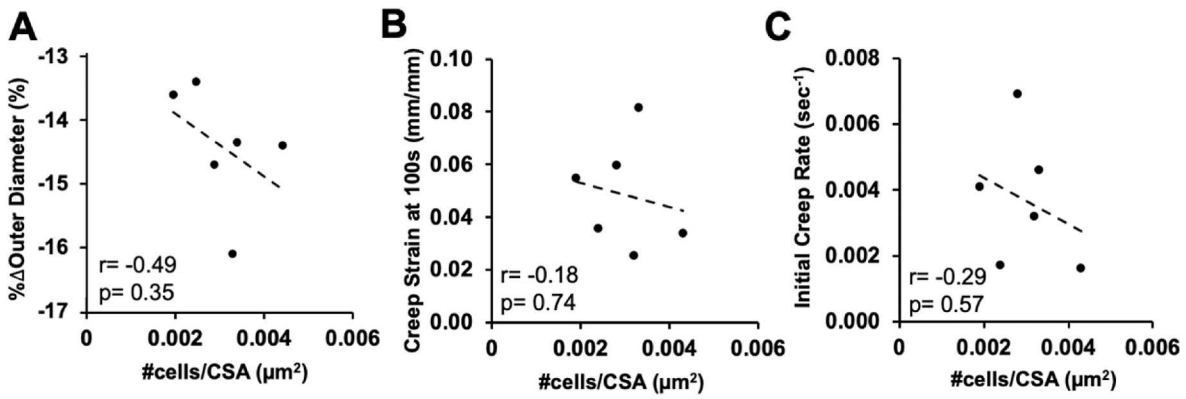

Fig. 9. Number of cells normalized to the muscularis cross-sectional area versus percent change in outer diameter with contractility (A). Number of cells normalized to the muscularis cross-sectional area versus creep strain at 100 s (B). Number of cells normalized to the muscularis cross-sectional area versus initial creep rate (C). The dashed line represents the best-fit line for the correlation.

increased with pressure. This suggests that with smooth muscle tone, the creep behavior was more sensitive to changes in pressure. Furthermore, that SMCs may play a role in maintaining vaginal diameter depending on the biomechanical environment. The contractile response also correlated with creep strain and rate for pressure-dependent active creep. As previously observed in the murine vagina, contractility decreased significantly with increased pressure (Clark et al., 2019). This suggests that the increase in pressure decreased the contractile response, which may have subsequently decreased creep.

While the phenomena observed in this study is interesting. It is not clear why creep increases with SMC activation and decreases with applied pressure. Future work leveraging other experimental animal models such as a diseased or aged tissue can provide a robust dataset to develop a mathematical model to further investigate this. Prior work presented a structural constitutive model that described the active and passive mechanical responses of biological tissues containing SMCs (Tan and De Vita, 2015). While this model provided valuable information to the field, it did not account for the multiaxial viscoelastic response of tissues. In the future, sufficient robust experimental data is needed to develop and validate a mathematical model that capture the multiaxial, anisotropic, viscoelastic, active, and passive properties of vaginal tissue.

This study did not identify a correlation between the number of smooth muscles cells and contractility (% change in outer diameter). Further, this study did not identify a relationship between the number of smooth muscles cells and creep (i.e., strain and rate) when maximally contracted with 40 mM KCl. This may be due to this study only quantifying the number of cells that expressed smooth muscle contractile proteins using a representative cross-section. Other factors may contribute to contractile behavior and smooth muscle contribution to creep that could not be captured with this analysis. This study focused on the expression of contractile proteins α SMA and/or MHC, but there are several limitations. The analysis assumed that all visualized cells are along the circumferential plane, however, some cell may be out of the plane (i.e., oriented axially) (Huntington et al., 2022). Secondly, the presence or number of contractile proteins may not be the only factors that contributes to smooth muscle contraction. The analysis did not evaluate smooth muscle phenotype and the colocalization of contractile proteins α SMA and MHC. Lastly, the model used in this study was a healthy nulliparous mouse. Therefore, the cell number may not vary much between samples. Future work evaluating active creep in a diseased, aged, or pregnant model will serve as a tool to further evaluate the relationship between active creep and the number of smooth muscle cells. Further, this will aid in developing a mathematical tool to elucidate why creep increases with smooth muscle cell activation and decreases with applied pressure.

In the murine vagina, the contractile response to 40 mM KCl resulted in a tonic contractile response where the outer diameter immediately decreased and remained relatively constant, as previously observed (Clark et al., 2019). When the vagina was contracted with 20 mM KCl, spontaneous contractions were observed, most often immediately after increasing pressure to 7 mmHg. While the vagina was separated from the cervix at the cervo-vaginal junction and tracked at the mid-anterior vaginal wall, cervical SMCs may have contributed to this response. For example, maximum contraction of the murine cervix is induced with 20 mM KCl (Conway et al., 2021), resulting in a phasic contractile response consisting of cyclic periods of contraction and relaxation. The frequency of phasic response, however, decreased to 0 Hz (tonic contractions) when the cervix was stimulated with 40 mM KCl (Conway et al., 2021). In the study by Conway et al. the vaginal fornix was still attached to the cervix, suggesting that at higher doses of KCl, the vagina dominates contractile behavior (Conway et al., 2021).

Together, these findings suggest that some of the vaginal samples were excised such that the cervical tissue might have contributed to spontaneous contractile behavior at 20 mM KCl. Additionally, studies demonstrated that mechanical stretch induced contraction in stomach SMCs (Kirber et al., 1988). This suggests that at certain concentrations of KCl stimulation, the vaginal SMCs may be sensitive to mechanical stretch resulting in spontaneous contractions. Alternatively, the local release of vasodilators such as nitric oxide may also contribute (Onol et al., 2006). Robust mechanistic studies are needed to evaluate this, and future work is needed to compare the contractile properties of the individual reproductive organs (e.g., vagina, cervix, and uterus), pelvic floor musculature and the entire reproductive system by evaluating the collective behavior.

This study is not without limitations. Creep was evaluated only along the circumferential direction; however, human studies suggest that SMCs are oriented along the circumferential and axial directions (Boreham et al., 2002; Siltberg et al., 1995). A recent study quantified the distribution of vaginal SMCs in the rat vagina (Huntington et al., 2022). In the proximal region of the rat vagina, more SMCs were oriented along the longitudinal (e.g., axial) than in the circumferential direction (Huntington et al., 2022). The immunofluorescent images presented in this study indicate that murine vaginal SMCs may be oriented along the circumferential and axial directions in the murine vagina. SMCs near the adventitia layer were elongated along the circumferential plane, whereas the cells near the subepethelium were more circular. The circular morphology may suggest that this is the cross-section of the cell, thus the cell was oriented axially. Alternatively, the circular morphology may suggest that the cell was more synthetic (e.g., less contractile) (Beamish et al., 2010).

Previous studies have demonstrated that in response to KCl axial contractility was greater than circumferential contractility in the rodent vagina (Clark et al., 2019; Huntington et al., 2018, 2021). Based on the findings of this and prior studies, creep may be greater in the axial

direction compared with the circumferential direction with smooth muscle contraction. It has also been hypothesized that in the axial direction, pressure may not significantly affect the active creep response. An earlier study demonstrated that increased pressure did not significantly affect axial contractility (Clark et al., 2019). Future work, however, is needed to evaluate creep circumferentially and axially to support or refute these hypotheses. The limited ability to assess creep axially in this study is attributed to the system being fixed axially and only tracking deformation along the circumferential direction. The use of an inflation device that allows free axial extension, as well as the use of optical imaging techniques such as digital image correlation, would permit quantifying creep both circumferentially and axially as recently done by Dubik et al. (2022). Despite this limitation, this study provided methods and valuable information on the contribution of SMCs to creep along the circumferential direction. To the authors' knowledge, this is the first study evaluating creep in the vagina following stimulation with various concentrations of chemical stimuli.

This study is also limited by the exclusive use of potassium chloride to induce smooth muscle contraction. This chemical surpasses complex mechanisms for contraction by directly depolarizing the cell-membrane. In addition to SMCs and extracellular matrix proteins, the vagina contains nerves for innervation (Jallah et al., 2016; Mazloomdoost et al., 2017, van Helden et al., 2017; Northington et al., 2011), and SMCs have receptors for the neurotransmitters that are released by localized nerves. Therefore, smooth muscle contraction can be induced *in vitro* by receptor agonist and nerve stimulation with electric field stimulation. SMCs in the murine vagina can also be stimulated with hormones such as oxytocin that induce a phasic contractile response (Gravina et al., 2014). Phasic contractile behavior was also present in the murine vagina depending on the anatomical region when using a receptor agonist (e.g., phenylephrine) and depending on the frequency when using nerve stimulation (van Helden et al., 2017). A previous study demonstrated that potassium chloride induced a tonic contractile response in all regions of the murine vagina (Clark et al., 2019; Gravina et al., 2014). Therefore, potassium chloride was selected for this study because a constant muscle contraction was critical to assess creep. A phasic contractile response will result in the diameter fluctuating through the creep test, affecting data analysis. This study provides a foundation for evaluating active creep in the vagina. Future work is needed to identify analytical methods to evaluate the vaginal creep in response to other stimuli that produce a phasic contractile response and to extend the methods developed in this study to other tubular reproductive organs that display phasic contractions such as the cervix and uterus.

5. Conclusion

This study presented methods to quantify the contribution of the SMCs to creep using various levels of potassium chloride and evaluated the contribution of smooth muscle to creep under an increased sustained pressure. Together, these studies demonstrated that SMC significantly increased viscoelastic behavior in the murine vagina compared with the passive (relaxed) state, the amount of contraction dictated the rate and degree of deformation under constant pressure, and that an increase in pressure significantly decreased contractility and decreased the active creep response. These results suggest that the SMCs provide mobility by allowing the vagina to stretch under sustained pressures. However, when pressure increases, the SMCs may resist deformation, providing stability to the vagina. In a healthy vagina, this may be critical for accommodating the dynamic pressures the vagina experiences with daily activities such as lying down, walking, and running (Kruger et al., 2013; Shaw et al., 2014).

To the authors' knowledge, this is the first experimental study evaluating smooth muscle contribution to creep (viscoelasticity) with varied pressure in a soft tissue. The methods developed in this study can serve as a tool to evaluate vaginal smooth muscle contribution to creep with pregnancy and aging, and in other tubular soft tissues. This experimental data set will permit the development of a mathematical model that describes and predicts not only the multiaxial active response of the vaginal tissue (as done in (Tan and De Vita, 2015)) but also the nonlinear viscoelasticity of such tissue to better understand physiological and pathophysiological processes in women's reproductive health.

Funding

This work was funded by the National Science Foundation [CMMI-1751050 (KSM), CMMI-2053851 (RD)] and National Institute of Health [HL155841 (BO), NIH R01 Award HL133619 (SHL)].

Data accessibility

The raw data is available at Github (https://github.com/bgandrlab/VaginalActiveCreep.git).

CRediT authorship contribution statement

Gabrielle L. Clark-Patterson: Writing – original draft, Methodology, Investigation, Formal analysis, Conceptualization. **Lily M. Buchanan:** Writing – original draft, Visualization, Formal analysis. **Benard O. Ogola:** Writing – original draft, Investigation. **Maria Florian-Rodriguez:** Writing – review & editing. **Sarah H. Lindsey:** Writing – review & editing. **Raffaella De Vita:** Writing – review & editing, Methodology, Funding acquisition, Conceptualization. **Kristin S. Miller:** Writing – review & editing, Supervision, Methodology, Funding acquisition, Conceptualization.

Declaration of competing interest

The authors declare that they have no known competing financial interests or personal relationships that could have appeared to influence the work reported in this paper.

Data availability

After acceptance data will be available at GitHub with the link.

Acknowledgments:

We acknowledge Claire Sentilles for developing the manual cell counting MATLAB code.

References

Akintunde, A., Robison, K.M., Capone, D., Desrosiers, L., Knoepp, L.R., Miller, K.S., 2019. Effects of elastase digestion on the murine vaginal wall biaxial mechanical response. J. Biomech. Eng. 141 (2).

Amin, M., Le, V.P., Wagenseil, J.E., 2012. Mechanical testing of mouse carotid arteries: from newborn to Adult. Jove-Journal of Visualized Experiments (60), 9.

Asundi, K.R., Rempel, D.M., 2008. MMP-1, IL-1 beta, and COX-2 mRNA expression is modulated by static load in rabbit flexor tendons. Ann. Biomed. Eng. 36 (2), 237–243.

Beamish, J.A., He, P., Kottke-Marchant, K., Marchant, R.E., 2010. Molecular regulation of contractile smooth muscle cell phenotype: implications for vascular tissue engineering. Tissue Eng. B Rev. 16 (5), 467–491.

Boreham, M.K., Wai, C.Y., Miller, R.T., Schaffer, J.I., Word, R.A., 2002. Morphometric analysis of smooth muscle in the anterior vaginal wall of women with pelvic organ prolapse. Am. J. Obstet. Gynecol. 187 (1), 56–63.

Bortolini, M.A.T., Shynlova, O., Drutz, H.P., Castro, R.A., Girao, M., Lye, S., Alarab, M., 2012. Expression of genes encoding smooth muscle contractile proteins in vaginal tissue of women with and without pelvic organ prolapse. Neurourol. Urodyn. 31 (1), 109–114.

Byers, S.L., Wiles, M.V., Dunn, S.L., Taft, R.A., 2012. Mouse estrous cycle identification tool and images. PLoS One 7 (4), 5.

Caulk, A.W., Humphrey, J.D., Murtada, S.I., 2019. Fundamental roles of axial stretch in isometric and isobaric evaluations of vascular contractility. Journal of Biomechanical Engineering-Transactions of the Asme 141 (3), 10.

Clark, G.L., Pokutta-Paskaleva, A.P., Lawrence, D.J., Lindsey, S.H., Desrosiers, L., Knoepp, L.R., Bayer, C.L., Gleason, R.L., Miller, K.S., 2019. Smooth muscle regional contribution to vaginal wall function. Interface Focus 9 (4), 13.

Clark, G.L., McGuire, J., Desrosiers, L., Knoepp, L.R., De Vita, R., Miller, K.S., 2021. Investigation of murine vaginal creep response to Altered mechanical loads. J. Biomech. Eng. 143 (12), 121008.
Clark-Patterson, G.L., McGuire, J., Desrosiers, L., Knoepp, L.R., De Vita, R., Miller, K.S., 2021. Investigation of murine vaginal creep response to Altered mechanical loads. J. Biomech. Eng. 143 (12).
Conway, C.K., Varghese, A., Mahendroo, M., Miller, K.S., 2021. The role of biaxial loading on smooth muscle contractility in the nulliparous murine cervix. Ann. Biomed. Eng. 49 (8), 1874–1887.
Daucher, J.A., Clark, K.A., Stolz, D.B., Meyn, L.A., Moalli, P.A., 2007. Adaptations of the rat vagina in pregnancy to accommodate delivery. Obstet. Gynecol. 109 (1), 128–135.
Dubik, J., Tartaglione, A., Miller, K.S., Dillard, D.A., De Vita, R., 2022. History-dependent deformations of rat vaginas under inflation. Integr. Comp. Biol. 62 (3), 625–640.
Ferruzzi, J., Bersi, M.R., Humphrey, J.D., 2013. Biomechanical phenotyping of central arteries in health and disease: Advantages of and methods for murine models. Ann. Biomed. Eng. 41 (7), 1311–1330.
Fox, C.A., Wolff, H.S., Baker, J.A., 1970. Measurement of intra-vaginal and intra-uterine pressures during human coitus by radio-telemetry. J. Reprod. Fertil. 22 (2), 243–251.
Fritze, O., Romero, B., Schleicher, M., Jacob, M.P., Oh, D.Y., Starcher, B., Schenke-Layland, K., Bujan, J., Stock, U.A., 2012. Age-related changes in the elastic tissue of the human Aorta. J. Vasc. Res. 49 (1), 77–86.
Gravina, F.S., van Helden, D.F., Kerr, K.P., de Oliveira, R.B., Jobling, P., 2014. Phasic contractions of the mouse vagina and cervix at different phases of the estrus cycle and during late pregnancy. PLoS One 9 (10), 9.
Greven, K., Hohorst, B., 1975. Creep after loading in relaxed and contracted (KC1 or K2SO4 depolarized) smooth muscle (taenia coli of the guinea pig). Pflügers Archiv 359 (1–2), 111–125.
Greven, K., Rudolph, K.H., Hohorst, B., 1976. Creep after loading in the relaxed and contracted smooth muscle (taenia coli of the guinea pig) under various osmotic conditions. Pflügers Archiv 362 (3), 255–260.
Hendrix, S.L., Clark, A., Nygaard, I., Aragaki, A., Barnabei, V., McTiernan, A., 2002. Pelvic organ prolapse in the women's health initiative: gravity and gravidity. Am. J. Obstet. Gynecol. 186 (6), 1160–1166.
Hingorani, R.V., Provenzano, P.P., Lakes, R.S., Escarcega, A., Vanderby, R., 2004. Nonlinear viscoelasticity in rabbit medial collateral ligament. Ann. Biomed. Eng. 32 (2), 306–312.
Hong, S.H., Kyeong, K.-S., Ji, I.W., Jeong, E.-H., Kim, H.S., Hwang, B.Y., Lee, C., Son, S. M., Kim, Y.C., You, R.Y., Lee, S.J., Na, K., Xu, W.-X., 2019. Regulation of murine myometrial contraction by ginger extract via activation of voltage dependent Ca 2+ channels. Biomed J Sci & Tech Res 20 (4), 15320–15327.
Huntington, A., Rizzuto, E., Abramowitch, S., Del Prete, Z., De Vita, R., 2018. Anisotropy of the passive and active rat vagina under biaxial loading. Ann. Biomed. Eng. 47 (1), 272–281.
Huntington, A., Abramowitch, S.D., Moalli, P.A., De Vita, R., 2021. Strains induced in the vagina by smooth muscle contractions. Acta Biomater. 129, 178–187.
Huntington, A.J., Udayasuryan, B., Du, P., Verbridge, S.S., Abramowitch, S.D., De Vita, R., 2022. Smooth muscle organization and nerves in the rat vagina: a first look using tissue clearing and immunolabeling. Ann. Biomed. Eng. 50 (4), 440–451.
Jallah, Z., Liang, R., Feola, A., Barone, W., Palcsey, S., Abramowitch, S.D., Yoshimura, N., Moalli, P., 2016. The impact of prolapse mesh on vaginal smooth muscle structure and function. Bjog-an International Journal of Obstetrics and Gynaecology 123 (7), 1076–1085.
Jorgensen, S., Hein, H.O., Gyntelberg, F., 1994. Heavy lifting at work and risk of genital prolapse and herniated lumbar disc in assistant nurses. Occupational Medicine-Oxford 44 (1), 47–49.
Kirber, M.T., Walsh, J.V., Singer, J.J., 1988. STRETCH-ACTIVATED ION channels in smooth-muscle - a mechanism for the initiatION of stretch-induced contractION. Pflueg. Arch. Eur. J. Physiol. 412 (4), 339–345.
Kruger, J., Hayward, L., Nielsen, P., Loiselle, D., Kirton, R., 2013. Design and development of a novel intra-vaginal pressure sensor. International Urogynecology Journal 24 (10), 1715–1721.
Mazloomdoost, D., Westermann, L.B., Mutema, G., Crisp, C.C., Kleeman, S.D., Pauls, R. N., 2017. Histologic anatomy of the anterior vagina and Urethra. Female Pelvic Med. Reconstr. Surg. 23 (5), 329–335.
Meston, C.M., Levin, R.J., Sipski, M.L., Hull, E.M., Heiman, J.R., 2004. Women's orgasm. Annu. Rev. Sex Res. 15, 173–257.
Murtada, S.I., Ferruzzi, J., Yanagisawa, H., Humphrey, J.D., 2016. Reduced biaxial contractility in the descending thoracic Aorta of Fibulin-5 deficient mice. Journal of Biomechanical Engineering-Transactions of the Asme 138 (5), 7.
Northington, G.M., Basha, M., Arya, L.A., Wein, A.J., Chacko, S., 2011. Contractile response of human anterior vaginal muscularis in women with and without pelvic organ prolapse. Reprod. Sci. 18 (3), 296–303.
Onol, F.F., Ercan, F., Tarcan, T., 2006. The effect of ovariectomy on rat vaginal tissue contractility and histomorphology. J. Sex. Med. 3 (2), 233–241.
Pack, E., Dubik, J., Snyder, W., Simon, A., Clark, S., De Vita, R., 2020. Biaxial stress relaxation of vaginal tissue in pubertal gilts. Journal of Biomechanical Engineering-Transactions of the Asme 142 (3), 7.
Peleg, M., 1979a. A model for creep and early Failure. Mater. Sci. Eng., A 40, 197–205.
Peleg, M., 1979b. Characterization of the stress relaxation curves of solid foods. J. Food Sci. 44 (1), 277–281.
Provenzano, P., Lakes, R., Keenan, T., Vanderby, R., 2001. Nonlinear ligament viscoelasticity. Ann. Biomed. Eng. 29 (10), 908–914.
Ramachandra, A.B., Humphrey, J.D., 2019. Biomechanical characterization of murine pulmonary arteries. J. Biomech. 84, 18–26.
Rempen, A., Kraus, M., 1991. Pressures on the fetal head during normal labor. J. Perinat. Med. 19 (3), 199–206.
Robison, K.M., Conway, C.K., Desrosiers, L., Knoepp, L.R., Miller, K.S., 2017. Biaxial mechanical assessment of the murine vaginal wall using extension-inflation testing. Journal of Biomechanical Engineering-Transactions of the Asme 139 (10), 8.
Rynkevic, R., Martins, P., Hympanova, L., Almeida, H., Fernandes, A.A., Deprest, J., 2017. Biomechanical and morphological properties of the multiparous ovine vagina and effect of subsequent pregnancy. J. Biomech. 57, 94–102.
S, T., 1973. Creep in glassy polymers. In: T*he Physics of Glassy Polymers*. Wiley, New York.
Shafik, A., El Sibai, O., Shafik, A.A., Ahmed, I., Mostafa, R.M., 2004. The electrovaginogram: study of the vaginal electric activity and its role in the sexual act and disorders. Arch. Gynecol. Obstet. 269 (4), 282–286.
Shafik, A., Shafik, I.A., El Sibai, O., Shafik, A.A., 2009. An electrophysiologic study of female ejaculation. J. Sex Marital Ther. 35 (5), 337–346.
Shaw, J.M., Hamad, N.M., Coleman, T.J., Egger, M.J., Hsu, Y., Hitchcock, R., Nygaard, I. E., 2014. Intra-abdominal pressures during activity in women using an intra-vaginal pressure transducer. J. Sports Sci. 32 (12), 1176–1185.
Siltberg, X.F.H., Johnson, P., Ulmsten, U., 1995. Viscoelastic properties and muscular function of the human anterior vaginal wall. International Urogynecology Journal 6 (4), 229–234.
Skoczylas, L.C., Jallah, Z., Sugino, Y., Stein, S.E., Feola, A., Yoshimura, N., Moalli, P., 2013. Regional differences in rat vaginal smooth muscle contractility and morphology. Reprod. Sci. 20 (4), 382–390.
Swift, S.E., Tate, S.B., Nicholas, J., 2003. Correlation of symptoms with degree of pelvic organ support in a general population of women: what is pelvic organ prolapse? Am. J. Obstet. Gynecol. 189 (2), 372–377.
Takacs, P., Gualtieri, M., Nassiri, M., Candiotti, K., Medina, C.A., 2008. Vaginal smooth muscle cell apoptosis is increased in women with pelvic organ prolapse. International Urogynecology Journal 19 (11), 1559–1564.
Tan, T., De Vita, R., 2015. A structural constitutive model for smooth muscle contraction in biological tissues. Int. J. Non Lin. Mech. 75, 46–53.
Thornton, G.M., Leask, G.P., Shrive, N.G., Frank, C.B., 2000. Early medial collateral ligament scars have inferior creep behaviour. J. Orthop. Res. 18 (2), 238–246.
Thornton, G.M., Boorman, R.S., Shrive, N.G., Frank, C.B., 2002. Medial collateral ligament autografts have increased creep response for at least two years and early immobilization makes this worse. J. Orthop. Res. 20 (2), 346–352.
Ulrich, D., Edwards, S.L., Su, K., White, J.F., Ramshaw, J.A.M., Jenkin, G., Deprest, J., Rosamilia, A., Werkmeister, J.A., Gargett, C.E., 2014. Influence of reproductive status on tissue composition and biomechanical properties of ovine vagina. PLoS One 9 (4), 8.
van Helden, D.F., Kamiya, A., Kelsey, S., Laver, D.R., Jobling, P., Mitsui, R., Hashitani, H., 2017. Nerve-induced responses of mouse vaginal smooth muscle. Pflueg. Arch. Eur. J. Physiol. 469 (10), 1373–1385.
Vanloon, P., Klip, W., Bradley, E.L., 1977. LENGTH-FORCE and volume-pressure relationships of arteries. Biorheology 14 (4), 181–201.
Vazquez-Padron, R.I., Lasko, D., Li, S., Louis, L., Pestana, I.A., Pang, M.H., Liotta, C., Fornoni, A., Aitouche, A., Pham, S.M., 2004. Aging exacerbates neointimal formation, and increases proliferation and reduces susceptibility to apoptosis of vascular smooth muscle cells in mice. J. Vasc. Surg. 40 (6), 1199–1207.
von Kleeck, R., Castagnino, P., Roberts, E., Talwar, S., Ferrari, G., Assoian, R.K., 2021. Decreased vascular smooth muscle contractility in Hutchinson-Gilford Progeria Syndrome linked to defective smooth muscle myosin heavy chain expression. Sci. Rep. 11 (1).
Wagner, H.P., Humphrey, J.D., 2011. Differential passive and active biaxial mechanical behaviors of muscular and elastic arteries: basilar versus common carotid. Journal of Biomechanical Engineering-Transactions of the Asme 133 (5), 10.
Wanggren, K., Stavreus-Evers, A., Olsson, C., Andersson, E., Gemzell-Danielsson, K., 2008. Regulation of muscular contractions in the human Fallopian tube through prostaglandins and progestagens. Hum. Reprod. 23 (10), 2359–2368.
Weizsacker, H.W., Lambert, H., Pascale, K., 1983. Analysis of the passive mechanical-properties of rat carotid arteries. J. Biomech. 16 (9), 703–715.
White, S.E., Conway, C.K., Clark, G.L., Lawrence, D.J., Bayer, C.L., Miller, K.S., 2019. Biaxial basal tone and passive testing of the murine reproductive system using a pressure myograph. Jove-Journal of Visualized Experiments (150), 13.